Application of Transient Electromagnetic Method for Mapping Deep-Seated Sulphide-Rich Zones in High-Resistivity Settings: A Case Study in Tsauni, Northcentral Nigeria

Abstract

The massive form of base metals in diverse geological settings holds greater economic significance than their disseminated counterparts, necessitating the distinction between massive and disseminated kinds. The sulphide mineralization in the area is recognized as hydrothermal vein-related rather than volcanogenic massive sulphide type, and it is situated in a highly resistive environment which prompted the use of TEM because of its capacity for depth penetration, it reduces electromagnetic coupling, improves resolution, is less sensitive to geological noise, and can acquire data faster; hence, the galvanic approach alone is insufficient for locating deep-seated sulphide-rich zones because of its limitations in current diffusion, electromagnetic coupling and depth limitations. Twenty-two (22) moving loops (Slingram) were established with dimensions of 200m by 200m. Simulations of individual lines conducted with Maxwell software indicated a substantial electromagnetic plate exhibiting a pronounced southerly dip, extensive strike, and significant depth extension. Following the fundamental initial hypothesis, this delineated the conductive structures associated with the deep-seated, sulphide-rich zone. The Tsauni sulphide deposit is observable along a 1 km strike length and demonstrates considerable conductivity indicative of tungsten sulphide potential. This process is particularly evident in regions where the host rock geology exhibits high resistivity; which is highly applicable in mineral Exploration, hydrocarbon Exploration and geothermal Exploration. The greater the resistivity, the more pronounced the induced polarisation relaxation impact on the transient electromagnetic signal.

Keywords: Tungsten, Base metals, Transient electromagnetic method (TEM), Tsauni.

Introduction

Rising apprehension in base-metal exploration, fuelled by anticipated future demand, has prompted the advancement of enhanced geophysical methodologies and sophisticated processing approaches for geophysical data. In base-metal exploration, TEM is a proficient geophysical technique that has been acknowledged as a significant factor in the discovery of volcanogenic massive sulphide (VMS) deposits during the past fifty years [1]; [2, 3]. The TEM facilitates the direct detection of VMS mineralization due to the elevated conductivity of the huge sulphides. The Transient Electromagnetic Method (TEM) is a time-domain electromagnetic exploration technique [4], extensively utilized in mineral exploration, geothermal studies, crustal structure analysis, and geophysical and engineering investigations. [5, 6] TEM detection is a crucial technique for metal detection. This paper aims to utilize TEM to detect BPC. The conventional TEM detection system primarily consists of

transmitting and receiving coils. [8] The pulse current is applied as the excitation source. [9] “While the current in the transmitting coil is quickly shut off, high di/dt causes a high magnetic field which is indicated as the “primary field”. Induced current, eddy or secondary current, is generated when a source magnetic field interacts with a subsurface ferromagnetic material. The time-varying secondary current also produces a new magnetic field referred to as the "secondary field." Eigenvalues derived from the secondary field can be utilized to ascertain the properties and position of certain objects”[12]. However, thanks to the inductive transmitting coil, the current in the transmitting coil does not abruptly go to zero after the switch is switched off [13]. “The residual primary field generated by that brief current will induce a disruptive voltage on the receiving voltage at the very early moment, which makes it impossible to obtain the pure signal induced by the secondary field. The limitations of the aforementioned transient transmission coil result in the neglect of early reception signals in conventional TEM detection, creating a detection blind zone within the range of 0 to 20 meters” [14, 15]. The depth of subterranean BPC is normally at 0~3 meters, which just falls in this detection blind zone. And as a result, interference from the primary field is inevitable. [16]

Site Location and Geology

The study region is within longitude 7^0 9’ 03’’ to 7^0 13’ 00’’ and latitude 9^0 17’ 04’’ to 9^0 22’ 07’’. Niger State is situated on the underlying complex rocks, and the remainder is comprised of the Cretaceous sedimentary rocks of the Bida Basin and a portion of the Sokoto (Iullemeden Basin). The basement rocks consist of a suite of Precambrian gneisses, migmatites, and metasedimentary schists crosscut by granitoids as shown in Figure 2. The migmatite-gneiss complex comprises migmatites, gneisses, mylonites, and amphibolites [17]. The mylonites are major shear zones that highlight the stratigraphic discontinuities between the gneissic basement complex and the overlying rocks of the Birnin-Gwari Schist formation. The schist belts area exists as two elongated masses separated by the older granite suite. The tops of the two formations are separated by a 40 km stretch of the older granite suite. However, one analysis finds a substantially lower separation of less than 10 miles. The Birnin-Gwari Formation rests to the west of the older granite (the Minna Batholith) while the Kushaka Formation lies to the East.

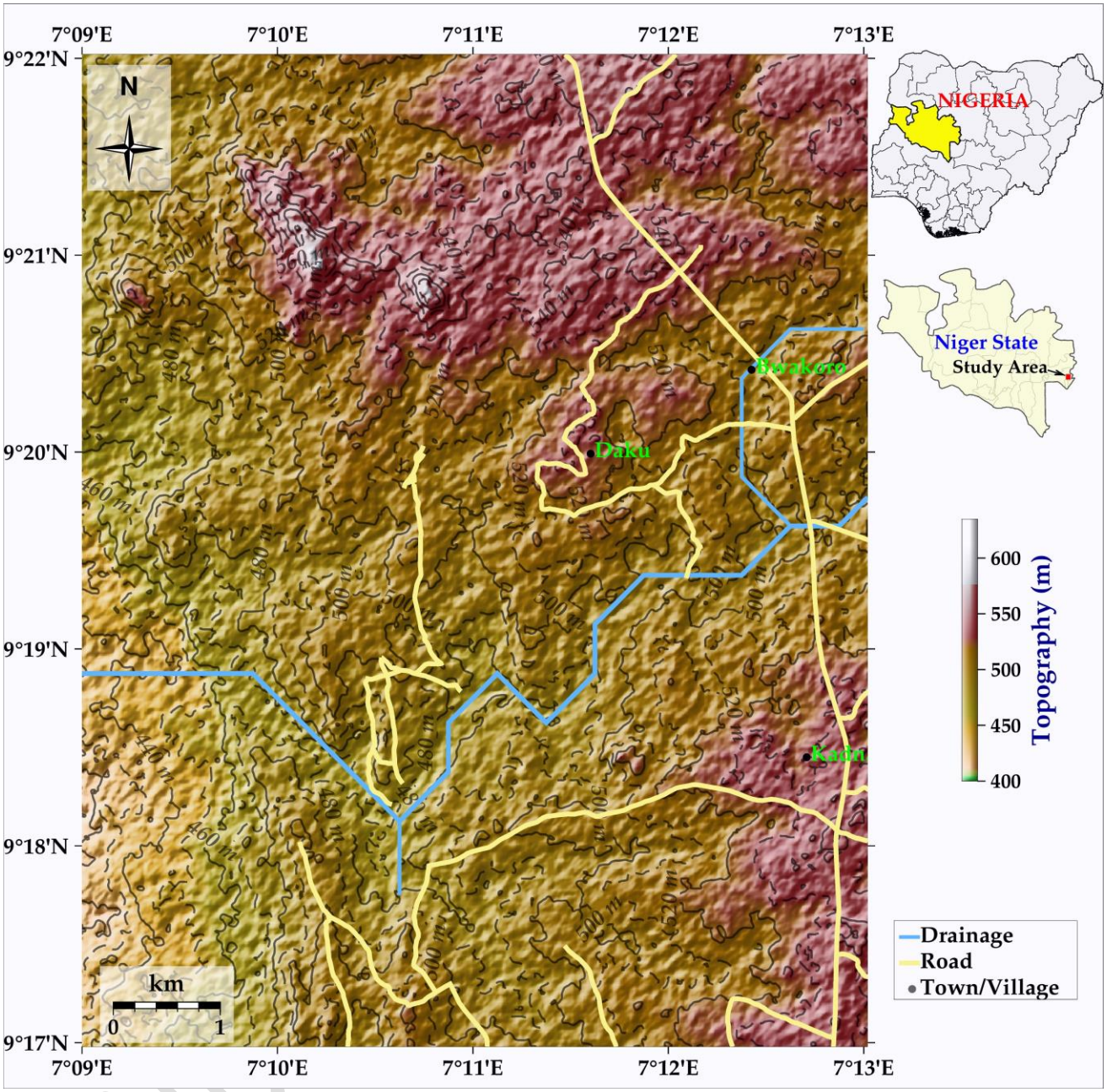

Figure 1: Location map of the study area

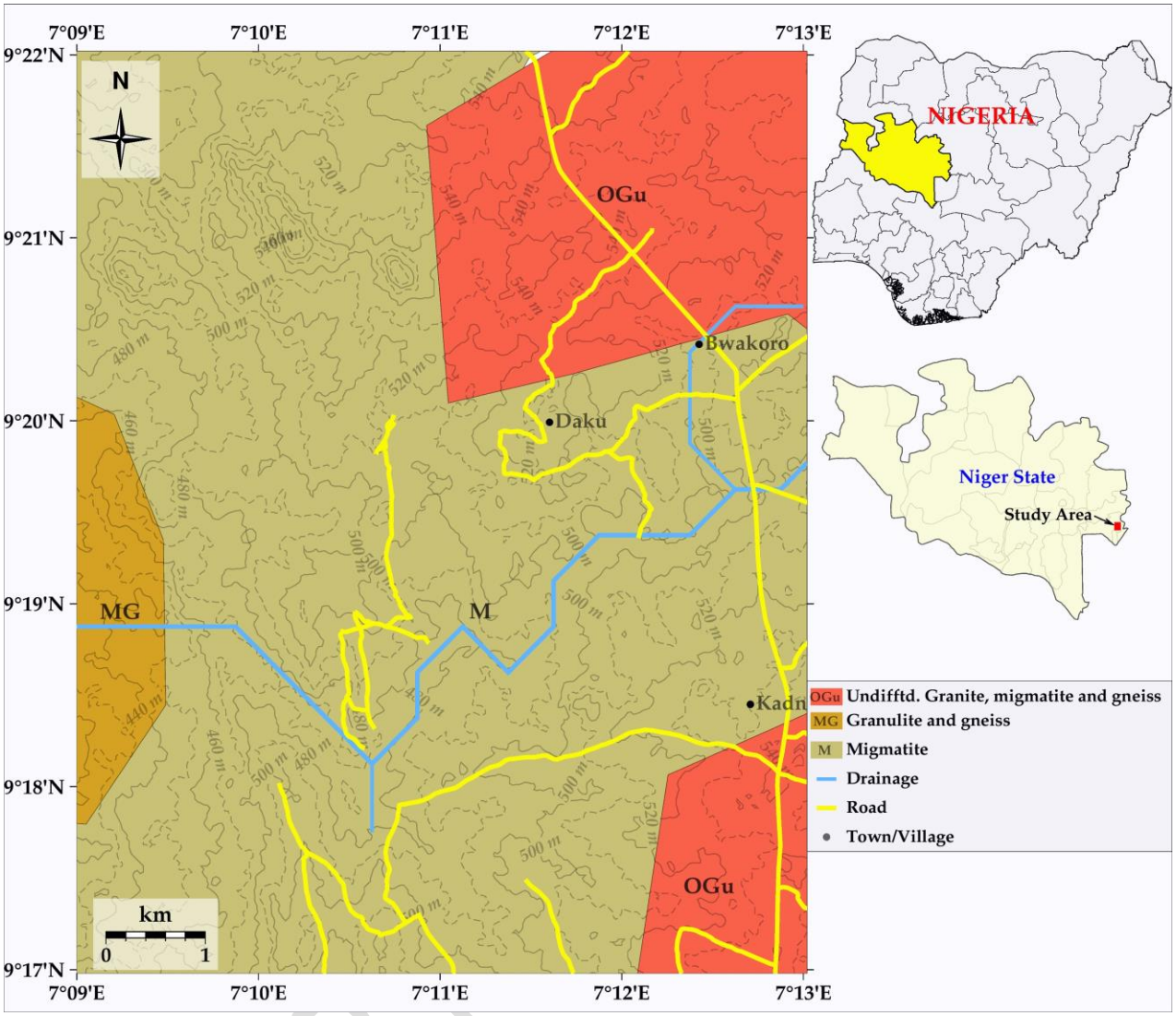

Figure 2: Geological map and Mineral Resources Map of the Study Area

Materials and Methods

A moving loop time domain ground EM survey was carried out over the key target area gained from the interpretation of ground magnetic data. The whole survey was conducted using a SMARTem24 receiver, 6 batteries connected in series powered Zonge ZT-30 transmitter capable of producing time-domain square waveforms into resistive loads that transmitted a 50% duty cycle square waveform at a base frequency of 50Hz into a 200m x 200m moving transmitter loop of 100m line spacing and 50m station spacing. “The transmitter controller was synchronized with the receiver using GPS. Readings were taken 100m beyond the loop, dubbed Slingram, at each station, and the Z component was measured. Since the transmitter loop for this mode went along the survey line at the same

time as the receiver at the back, the position of the loop changed with each station measured. Forward modeling was also carried out for the anticipated EM response". The data was examined with Maxwell software for possible dip angle, orientation, and conductive bodies.

Data Processing and Interpretation

The Late-time Constant

The Late-Time Constant (LTC) is an important measure in Transient Electromagnetic (TEM) surveys, representing the decay rate of the secondary electromagnetic field during late time intervals. The Late-time constants serve as an excellent tool for finding highly conductive anomalies without necessitating lateral plots of distinct channels. The measurements are made in time windows (or channels). The response from poor conductors is registered in early channels and the response from good conductors is registered in late channels. [17]. The temporal constant, Tau, specifies the decay rate of an exponential function, specifically the length needed for the signal to decline to 1/e (approximately 37%) of its initial size. In the context of TEM surveys, Tau signifies the duration necessary for induced currents to fall to about 37% of their initial strength following the cessation of the transmitter loop's source current. The late-time constant image (Figure 3) enhances the imaging of decay rates, enabling for the finding of conductive anomalies. LTC delineates the decay rate of the secondary field over late time periods (>10-20 ms), as shown in the configuration file of the survey (Figure 4), often expressed as:

$$\text{LTC } (\tau) = \tau = 1 / (\rho / \mu)$$

where:

τ = Late-Time Constant (s)

ρ = Resistivity of the subsurface (Ωm)

μ = Magnetic permeability (H/m)

LTC values can be interpreted as:

1. Low LTC (<10 ms): Shallow, conductive targets
2. Medium LTC (10-100 ms): Moderate-depth, moderate-conductivity targets
3. High LTC (>100 ms): Deep, resistive targets

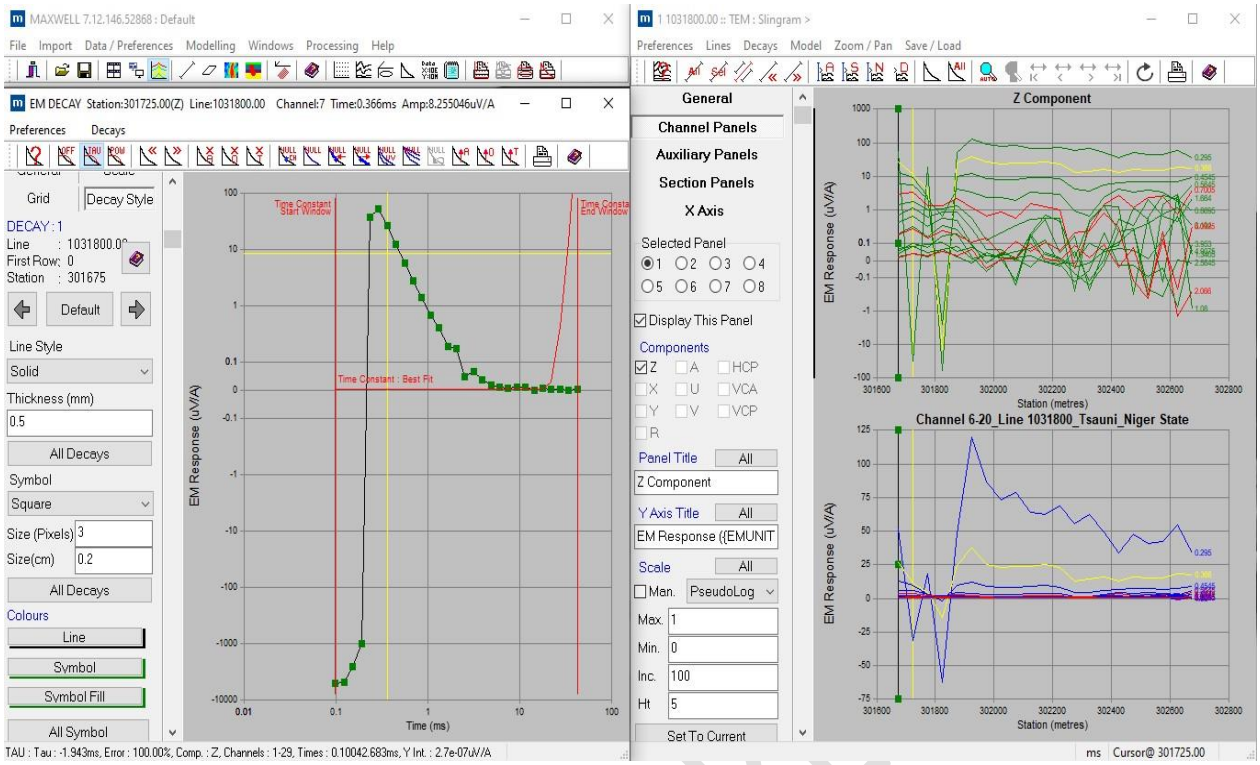

Figure 3: The moving loop data in Maxwell showing the decay curves at profile line 1031800 at channel 7

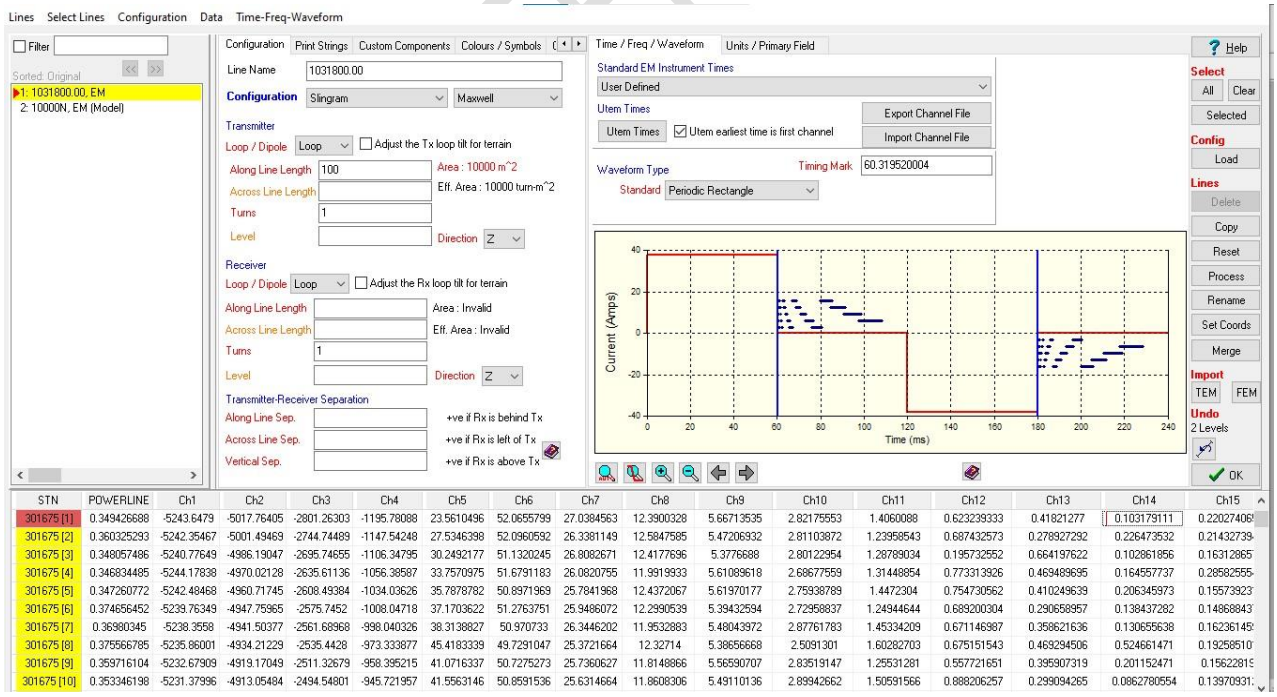

Figure 4: The Line editor dialog box for Maxwell which can be used to create a configuration file for the survey.

Moving Loop Time Domain Ground EM Survey Data

The SMARTem24 and Zonge ZT 30 devices offer data quality assessment in resistive host rocks that contain conductive entities or anomalies. The moving loop survey was configured with dimensions of 200m by 200m. Downloaded data were imported into the Maxwell application in either. DAT or. TEM format. Presenting data as profiles aids in easier anomaly identification. Figure 4 exhibits the imported data in Maxwell, with the right side presenting the EM response for a single line (Line 1031800) for the measured Z-component. Users can cycle across lines to analyse each EM response. Twenty-two (22) moving loop (Slingram) lines were individually simulated using Maxwell software, indicating a large EM plate with a steep southerly dip, extensive strike, and great deep extension, aligning with the basic starting model. Figure 5 demonstrates the modelling findings for four of these lines. The moving loop EM survey comprised a strike length of around 2km, with a line spacing of 50 meters and comparable station spacing. Subsequent forward modelling involved changing the plate parameters until the model response was closely aligned with the measured EM response, as displayed in Figure 5. In this photo, the black traces indicate the measured time-channel EM response, while the red traces show the calculated model response, allowing a visual contrast between the two.

The moving loop data modelling reveals a steeply dropping EM plate with a large strike and depth extension. However, no "resultant EMD` plates" were generated at the center of the large EM plates due to the moving loop data, as the conductance values (less than 100S) suggest that the method primarily mapped disseminated mineralization and limited massive sulphide mineralization within the granitic and schist rocks. This constraint is connected to the tiny transmitter loop size (200m x 200m), which resulted in a low dipole moment. In a moving loop setup for Transient Electromagnetic (TEM) data gathering, the only usage of the Z-component (vertical component) is often due to the following reasons

1. Simplification: Measuring simply the Z-component simplifies the data collecting process and decreases the amount of data to be processed.
2. Dominant response: The Z-component generally dominates the TEM response, especially in places with strong conductivity, providing the most relevant information about the subsurface.
3. Noise reduction: By focusing on the Z-component, noise, and interference from horizontal components (X and Y) are decreased, resulting in a cleaner signal.

4. Depth penetration: The Z-component is more sensitive to deeper structures, allowing for better depth penetration and imaging of subsurface objects.

5. Convention: It is a frequent convention in TEM surveys to employ the Z-component as the major or only component for data collecting and interpretation.

The dimensions of the plate are determined by factors such as strike length, which indicates the plate's width along the striking direction, and depth extent, which represents the plate's height along the dipping side. Given that the plate is deemed thin, its thickness and conductivity are closely related and cannot be measured independently. As a result, their product, known as conductivity thickness or conductance, is used to characterise the electrical properties of the thin conductor. The EM plate parameters for all 22 simulated loop lines are given in Table 1.

Line = Line number

E = UTM Easting of the CENTER TOP OF PLATE

N = UTM Northing of the CENTER TOP OF PLATE

Z= Elevation above GPS spheroid of the centre top of the plate in meters

Depth below ground level of the centre top of the plate in meters

Dip = Dip of the plate in dip direction (DD)

DD = Dip direction of the plate (perpendicular to geological strike)

SL = Strike length in meters

DE = Down-dip depth extent in meters

The Plate thickness in meters (for thick plates)

CT or Cd = CT is a conductivity-thickness product (Siemens) used for thin plates

Cd is a measure of conductivity for thick plates.

Channels = modelled Range of EM channels used in the inversion

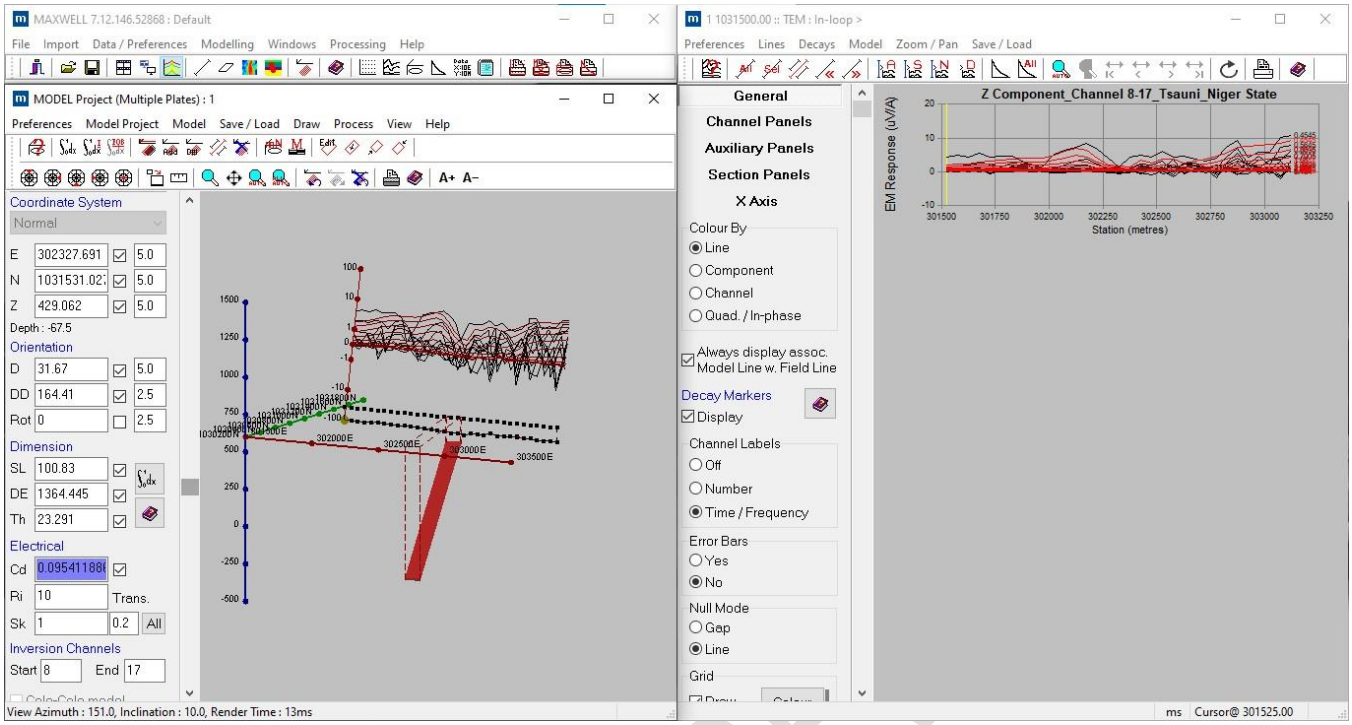
MAXWELL 7.12.146.52868 : Default
File Import Data / Preferences Modelling Windows Processing Help
MODEL Project (Multiple Plates) : 1
Preferences Model Project Model Save / Load Draw Process View Help
Coordinate System
Normal
E 302327.691 5.0
N 1031531.02 5.0
Z 429.062 5.0
Depth : -67.5
Orientation
D 31.67 5.0
DD 164.41 2.5
Rot 0 2.5
Dimension
SL 100.83
DE 1364.445
Th 23.291
Electrical
Cd 0.095411886
Pi 10 Trans.
Sk 1 0.2 All
Inversion Channels
Start 8 End 17
302000E
302500E
303000E
303500E
View Azimuth : 151.0, Inclination : 10.0, Render Time : 13ms
1 1031500.00 :: TEM : In-loop >
Preferences Lines Decays Model Zoom / Pan Save / Load
General
Channel Panels
Auxiliary Panels
Section Panels
X Axis
Colour By
Line
Component
Channel
Quad. / In-phase
Always display assoc. Model Line w. Field Line
Decay Markers
Display
Channel Labels
Off
Number
Time / Frequency
Error Bars
Yes
No
Null Mode
Gap
Line
Grid
Z Component_Channel 8-17_Tsauni_Niger State
EM Response (uV/A)
Station (metres)
ms Cursor@ 301525.00

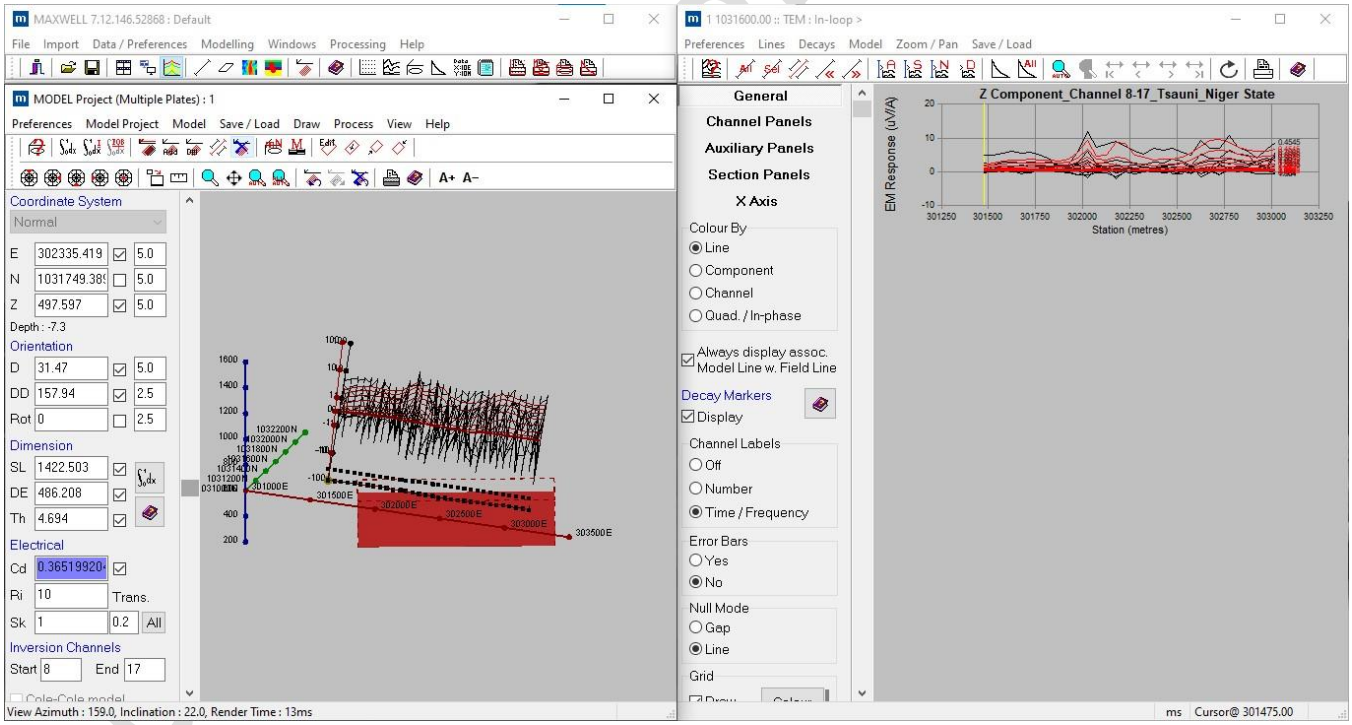
MAXWELL 7.12.146.52868 : Default
File Import Data / Preferences Modelling Windows Processing Help
MODEL Project (Multiple Plates) : 1
Preferences Model Project Model Save / Load Draw Process View Help
Coordinate System
Normal
E 302335.419 5.0
N 1031749.38 5.0
Z 497.597 5.0
Depth : -7.3
Orientation
D 31.47 5.0
DD 157.94 2.5
Rot 0 2.5
Dimension
SL 1422.503
DE 486.208
Th 4.694
Electrical
Cd 0.36519920
Pi 10 Trans.
Sk 1 0.2 All
Inversion Channels
Start 8 End 17
301500E
302000E
302500E
303000E
303500E
View Azimuth : 159.0, Inclination : 22.0, Render Time : 13ms
1 1031600.00 :: TEM : In-loop >
Preferences Lines Decays Model Zoom / Pan Save / Load
General
Channel Panels
Auxiliary Panels
Section Panels
X Axis
Colour By
Line
Component
Channel
Quad. / In-phase
Always display assoc. Model Line w. Field Line
Decay Markers
Display
Channel Labels
Off
Number
Time / Frequency
Error Bars
Yes
No
Null Mode
Gap
Line
Grid
Z Component_Channel 8-17_Tsauni_Niger State
EM Response (uV/A)
Station (metres)
ms Cursor@ 301475.00

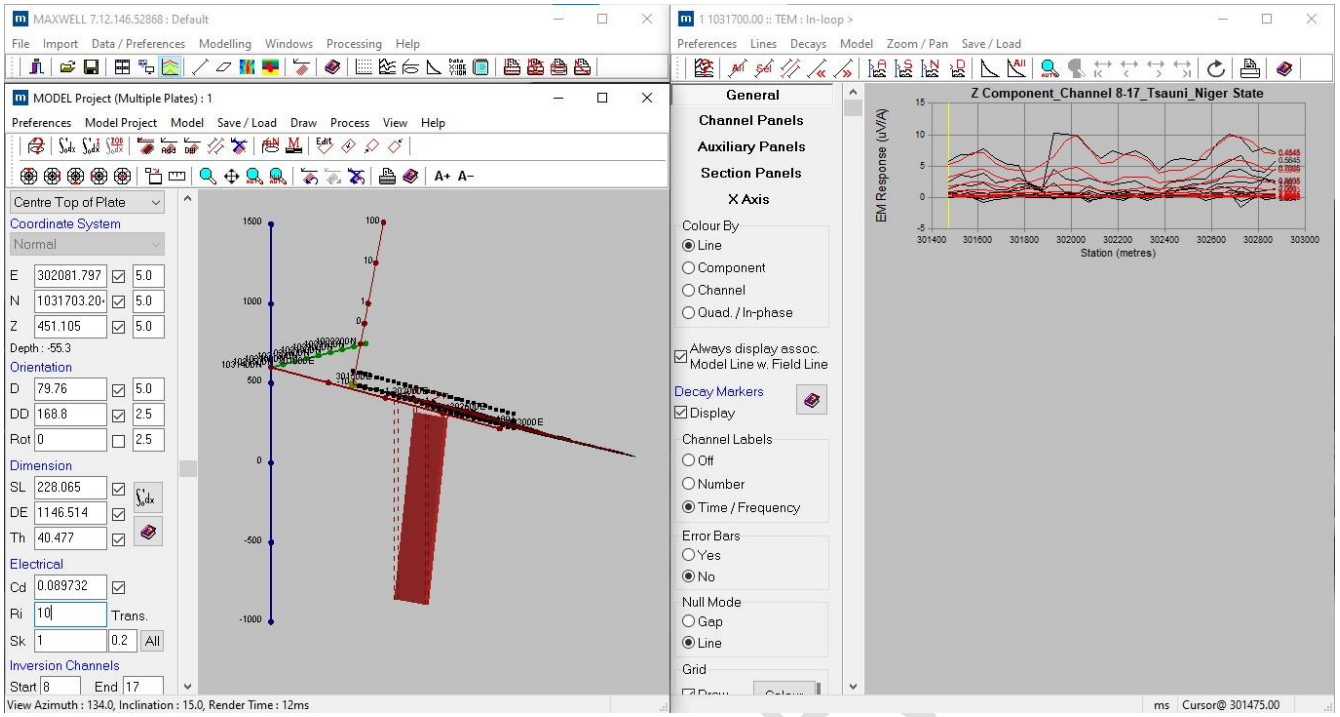
MAXWELL 7.12.146.52868 : Default
File Import Data / Preferences Modelling Windows Processing Help
MODEL Project (Multiple Plates) : 1
Preferences Model Project Model Save / Load Draw Process View Help
Centre Top of Plate
Coordinate System
Normal
E 302081.797 5.0
N 1031703.20 5.0
Z 451.105 5.0
Depth : -55.3
Orientation
D 79.76 5.0
DD 168.8 2.5
Rot 0 2.5
Dimension
SL 228.065
DE 1146.514
Th 40.477
Electrical
Cd 0.089732
Ri 10 Trans.
Sk 1 0.2 All
Inversion Channels
Start 8 End 17
View Azimuth : 134.0, Inclination : 15.0, Render Time : 12ms
1 1031700.00 :: TEM : In-loop >
Preferences Lines Decays Model Zoom / Pan Save / Load
General
Channel Panels
Auxiliary Panels
Section Panels
X Axis
Colour By
Line
Component
Channel
Quad. / In-phase
Always display assoc. Model Line w. Field Line
Decay Markers
Display
Channel Labels
Off
Number
Time / Frequency
Error Bars
Yes
No
Null Mode
Gap
Line
Grid
Z Component_Channel 8-17_Tsauni_Niger State
EM Response (uV/A)
Station (metres)
ms Cursor@ 301475.00

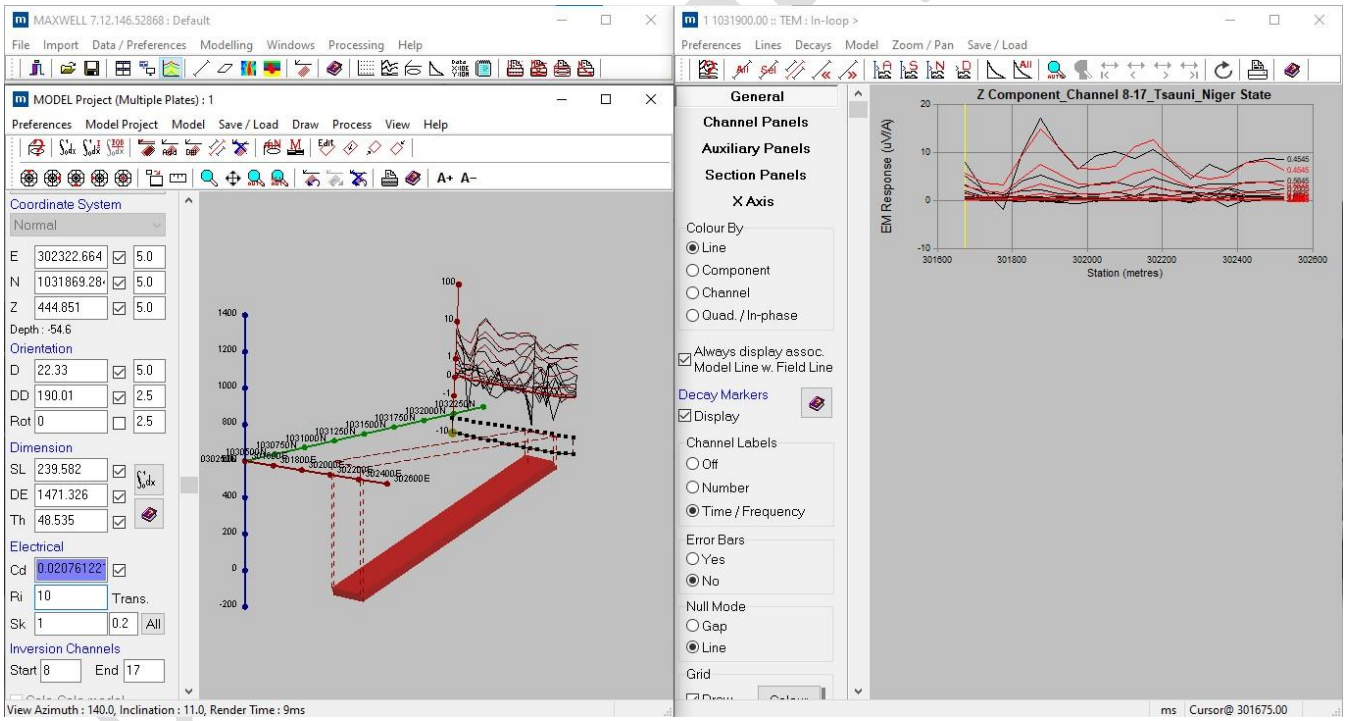
MAXWELL 7.12.146.52868 : Default
File Import Data / Preferences Modelling Windows Processing Help
MODEL Project (Multiple Plates) : 1
Preferences Model Project Model Save / Load Draw Process View Help
Coordinate System
Normal
E 302322.664 5.0
N 1031869.28 5.0
Z 444.851 5.0
Depth : -54.6
Orientation
D 22.33 5.0
DD 190.01 2.5
Rot 0 2.5
Dimension
SL 239.582
DE 1471.326
Th 48.535
Electrical
Cd 0.02076122
Ri 10 Trans.
Sk 1 0.2 All
Inversion Channels
Start 8 End 17
View Azimuth : 140.0, Inclination : 11.0, Render Time : 9ms
1 1031900.00 :: TEM : In-loop >
Preferences Lines Decays Model Zoom / Pan Save / Load
General
Channel Panels
Auxiliary Panels
Section Panels
X Axis
Colour By
Line
Component
Channel
Quad. / In-phase
Always display assoc. Model Line w. Field Line
Decay Markers
Display
Channel Labels
Off
Number
Time / Frequency
Error Bars
Yes
No
Null Mode
Gap
Line
Grid
Z Component_Channel 8-17_Tsauni_Niger State
EM Response (uV/A)
Station (metres)
ms Cursor@ 301675.00

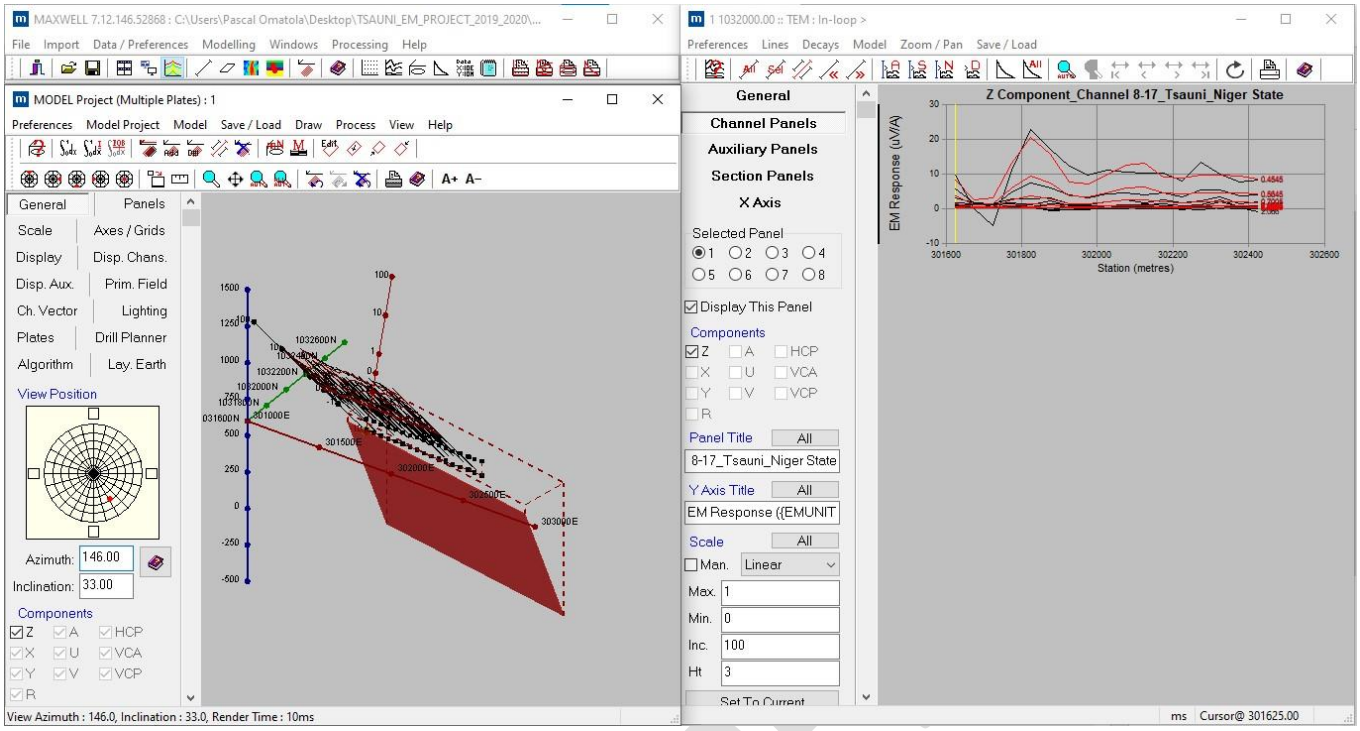
MAXWELL 7.12.146.52868 : C:\Users\Pascal Omatola\Desktop\TSAUNI_EM_PROJECT_2019_2020\...
File Import Data / Preferences Modelling Windows Processing Help
MODEL Project (Multiple Plates) : 1
Preferences Model Project Model Save / Load Draw Process View Help
General Panels
Scale Axes / Grids
Display Disp. Chans.
Disp. Aux. Prim. Field
Ch. Vector Lighting
Plates Drill Planner
Algorithm Lay. Earth
View Position
Azimuth: 146.00
Inclination: 33.00
Components
Z A HCP
X U VCA
Y V VCP
R
View Azimuth : 146.0, Inclination : 33.0, Render Time : 10ms
1 1032000.00 :: TEM : In-loop >
Preferences Lines Decays Model Zoom / Pan Save / Load
General
Channel Panels
Auxiliary Panels
Section Panels
X Axis
Selected Panel
1 2 3 4
5 6 7 8
Display This Panel
Components
Z A HCP
X U VCA
Y V VCP
R
Panel Title All
8-17_Tsauni_Niger State
Y Axis Title All
EM Response ({EMUNIT
Scale All
Man. Linear
Max. 1
Min. 0
Inc. 100
Ht 3
Set To Current
Z Component_Channel 8-17_Tsauni_Niger State
EM Response (uV/A)
Station (metres)
ms Cursor@ 301625.00

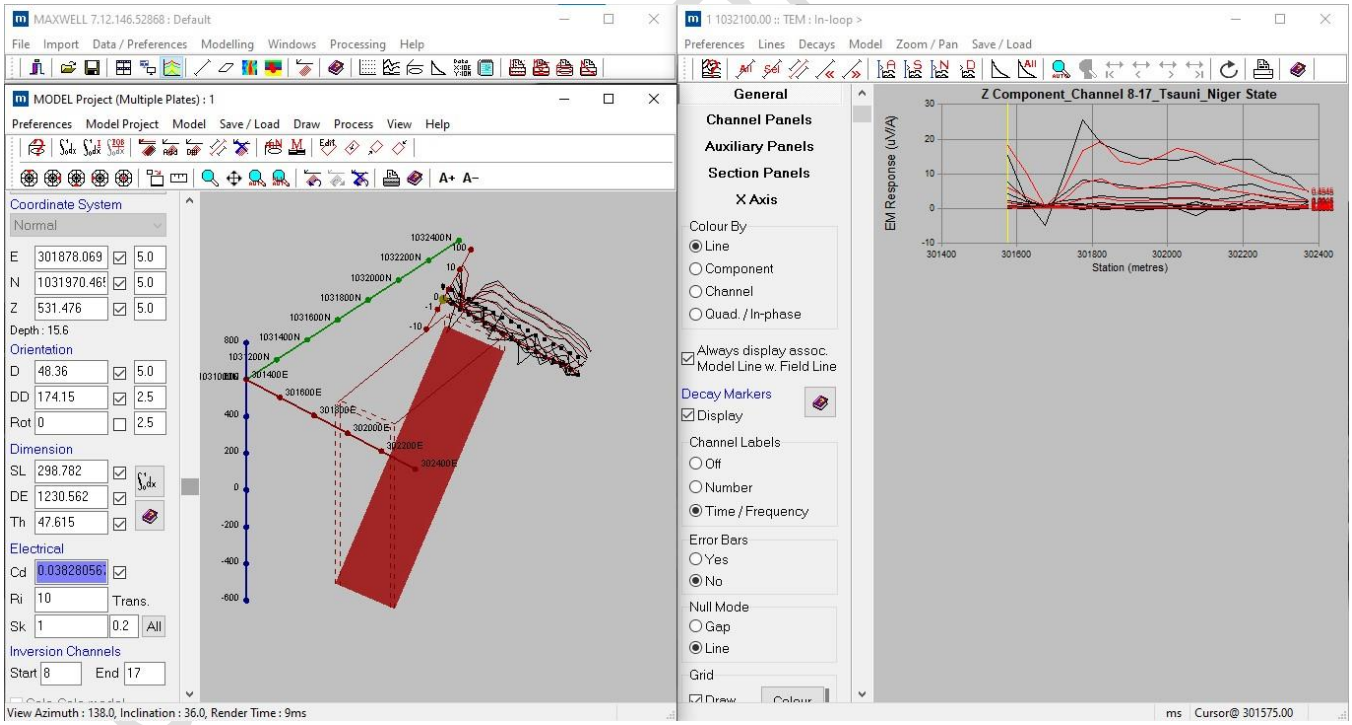
MAXWELL 7.12.146.52868 : Default
File Import Data / Preferences Modelling Windows Processing Help
MODEL Project (Multiple Plates) : 1
Preferences Model Project Model Save / Load Draw Process View Help
Coordinate System
Normal
E 301878.069 5.0
N 1031970.46 5.0
Z 531.476 5.0
Depth : 15.6
Orientation
D 48.36 5.0
DD 174.15 2.5
Rot 0 2.5
Dimension
SL 298.782
DE 1230.562
Th 47.615
Electrical
Cd 0.03828056
Ri 10 Trans.
Sk 1 0.2 All
Inversion Channels
Start 8 End 17
View Azimuth : 138.0, Inclination : 36.0, Render Time : 9ms
1 1032100.00 :: TEM : In-loop >
Preferences Lines Decays Model Zoom / Pan Save / Load
General
Channel Panels
Auxiliary Panels
Section Panels
X Axis
Colour By
Line
Component
Channel
Quad. / In-phase
Always display assoc. Model Line w. Field Line
Decay Markers
Display
Channel Labels
Off
Number
Time / Frequency
Error Bars
Yes
No
Null Mode
Gap
Line
Grid
Draw Colour
Z Component_Channel 8-17_Tsauni_Niger State
EM Response (uV/A)
Station (metres)
ms Cursor@ 301575.00

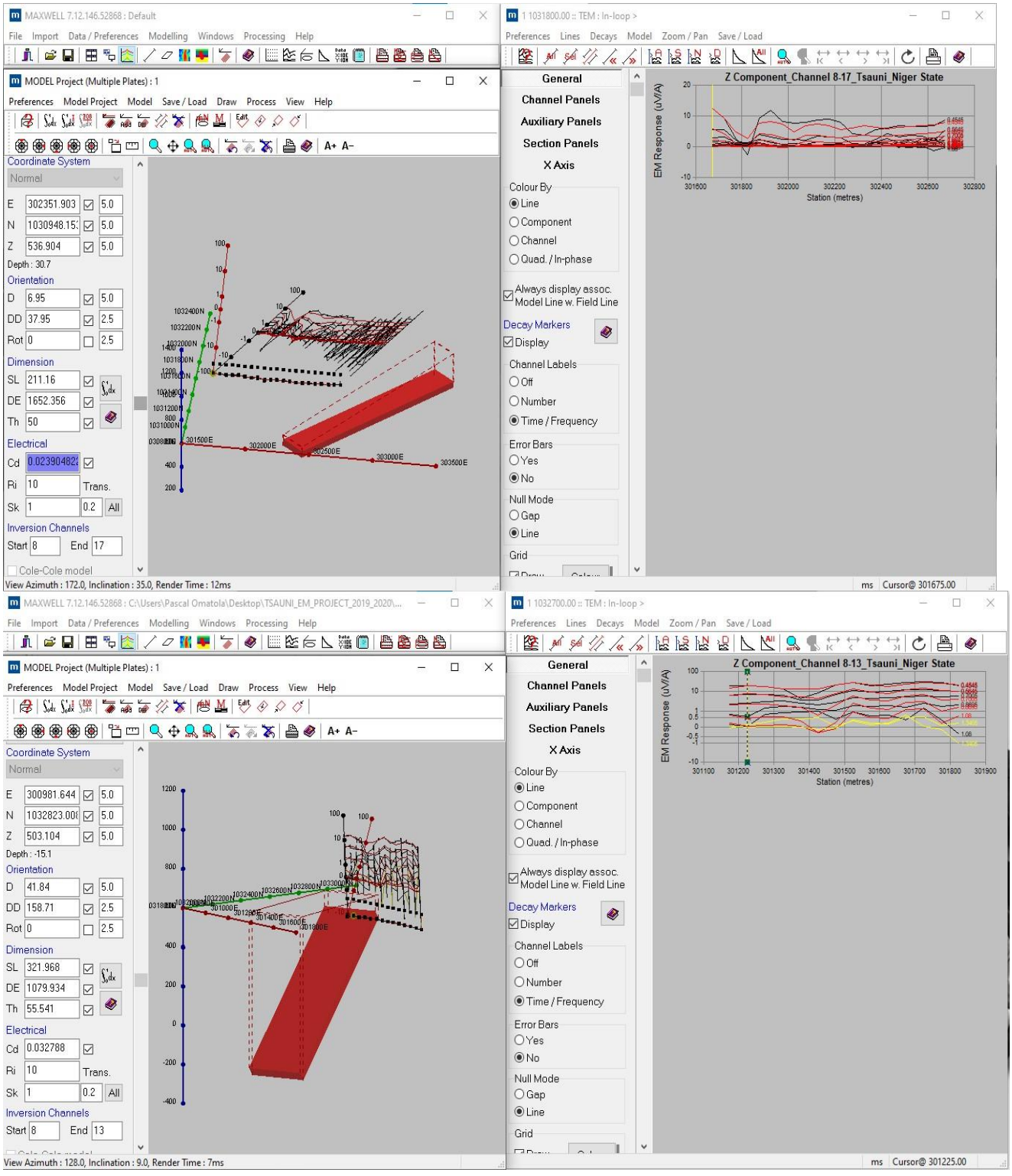

Figure 5: Modelling results for selected line profiles. The left window shows the modeled EM plate steeply dipping to the south correlating with the mineralized ultramafic sill. The right window depicts the measured EM response traces in black and the modeled EM response in red for the components Z

Table 1: EM plate parameters for all the modelled Loop lines

Line	Depth (m)	Dip	Dip Direction	Strike Length (m)	Depth Extent(m)	Thickness (m)	Conductance	Azimuth	Inclination
1031000	531.6	61	241.7	931.8	1848.2	41.9	0.053	154.0	30.0
1031200	198.5	46	179.7	340.0	1501.7	46.5	0.049	166.0	38.0
1031300	309.9	40	24.6	611.7	2641.1	39.5	0.045	121.0	17.0
1031400	32.4	56	15.4	392.2	880.5	44.4	0.033	158	20.0
1031500	67.5	32	164.4	100.8	1364.4	23.3	0.095	151	10.0
1031600	7.3	32	157.9	1422.5	486.2	4.7	0.365	159	22.0
1031700	55.3	80	168.8	228.1	1146.5	40.5	0.089	134	15.0
1031800	30.7	7	37.9	211.2	1652.4	50	0.024	172	35.0
1031900	54.6	22	190.0	239.6	1471.3	48.5	0.021	140	11.0
1032000	15.6	48	174.2	298.8	1230.6	47.6	0.038	138	36.0
1032200	3.9	11	162.0	398.7	1482.9	45.7	0.031	137	23.0
1032300	15.8	39	166.5	343.7	960.8	51.2	0.037	128	14,0
1032400	44.1	68	336.4	1379.4	1195.4	38.8	0.036	176	63.0
1032500	79.9	21	183.4	414.9	1322.8	77.2	0.026	131	30.0
1032600	42.9	90	352.7	1379.5	872.6	57.9	0.030	117	11.0
1032700	15.1	42	158.7	321.9	1079.9	55.5	0.033	128	9.0
1032800	8.3	18	179.7	857.1	1136.5	49.9	0.028	139	11.0

Results and Discussions

Interpretation of TEM Anomaly

All plates in the TEM model dip range from 11 degrees to 90 degrees with the highest dip direction of 336.4. The shallower plates have a conductivity-thickness product of 0.021 Siemens and the deeper plate has a C-T of about 0.365 Siemens with the highest strike length of 1422.5m. The major physical attribute of the inductive EM approaches used in this investigation is electrical conductivity. Because of the large physical discrepancy between the electrical properties of the well-mineralized vein and the host rocks, EMIT's Maxwell Electromagnetic software was employed in the modeling of all the ground EM data. Since the mineralized vein of Tsauni ultramafic intrusion is a steeply dipping sheet with a considerable strike and depth extension, so also the EM model plates. The simulated plates were very extensive with a strike extent of around 1km and a depth extent of 1.2 km sloping steeply to the south as shown in (Figure 6) aligning very well with the geology model of the mineralized ultramafic sill. To properly confine the targets, an assumption was made that at late decay times, the currents would be localized in the center of the big EM plate indicating the most conductive region of the intrusion. Smaller 'Resultant EM plates' of dimensions, 200x200m that coincide with the core of the huge EM plates (with a conductance less than 2 Siemens) where current will be directed at late decay times were therefore produced in Maxwell software. The physical property measurements (conductivity) were taken to indicate that the net-textured was well-mineralized.

TEM interpretation comprises two distinct approaches. The first strategy involves using profile data to find EM anomalies, while the second approach employs gridded data as shown in Figure 6, mainly from late-time channels and late-time constants, to generate images that enhance the interpretation of profile data. By combining these approaches, anomalies detected by the SMARTem24 electromagnetic system can be categorized into three major types: notably cultural, surficial, and bedrock:

1. Cultural conductors are caused by human-made constructions such as fences, power lines, buried pipes, and other metal objects. These structures can cause anomalies if they form closed conducting loops, either by being well-grounded in a conductive environment or due to their physical shape and geometry.
2. Surficial conductors are flat-lying conductors that occur on or just below the surface. The anomalies they generate are often broad, have poor conductivity, and are big in amplitude.

Examples include Quaternary cover and conductive regolith, which cause characteristic anomalies due to their shallow depth and extensive extent.

3. Bedrock conductors are often steeply dipping narrow targets of high conductivity embedded in a highly resistant host environment. Strike length may be large.

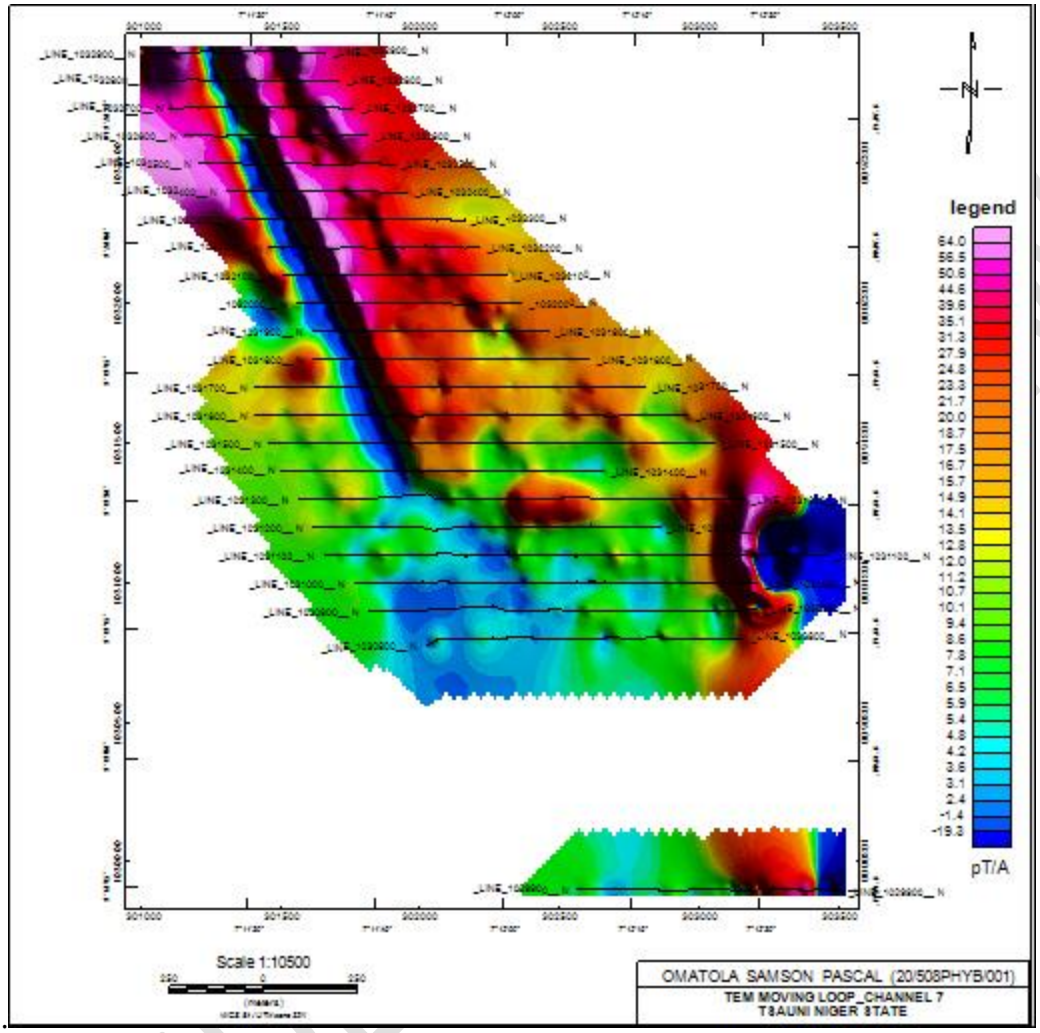

Figure 6: Channel 7 Z-component image of the moving loop mode mapping the conductive intrusion of the study area.

Conclusion

Twenty-two 200m-by-200m Slingrams were built. The Maxwell software simulations of various lines showed a massive electromagnetic plate with a southerly dip, extensive strike, and significant depth extension. Following the first premise, this revealed the deep-seated, sulphide-rich zone's conductive structures. Conductivity along a 1 km strike length of the Tsauni sulphide deposit suggests tungsten sulphide potential. In places with high host rock resistivity, this process is very visible.

The Tsauni sulphide body is observable along a 1km strike length, demonstrating considerable conductivity. Tsauni area is more conductive than the diffused mineralized copper, the created center of EM plates with conductivity thickness less than 2 Siemens were considered to imply the well-mineralized net-textured and huge sulphide stringers. Additionally, two known sulphide possibilities containing Tungsten were also discovered. Several substantial sedimentary sulphide deposits with great economic potential were discovered within the survey region

Disclaimer (Artificial intelligence)

Author(s) hereby declare that NO generative AI technologies such as Large Language Models (ChatGPT, COPILOT, etc.) and text-to-image generators have been used during the writing or editing of this manuscript.

References

[1]. Alan G., Galley, Hannington M.D., and Johnson, J.R., 2007: Volcanogenic massive sulphide deposits, Mineral deposits of Canada; A synthesis of major deposit type and exploration methods, Geological Association of Canada, Special Publication No. 5, p. 141-161.

[2]. Fritz, F.P., and Sheehan, G.M., 1984: The geophysical signature of the Teutonic Bore Cu-Zn-Ag massive sulphide deposit western Australia, Exploration Geophysics, Vol. 15, p. 127-142.

[3]. Gitonga, G., 2011: Geophysical techniques used in volcanogenic massive sulphide exploration in Archean Greenstone belt of western Kenya: Case study YALA-(KKAMEGA), dissertation thesis of B.Sc. degree, University of Nairobi.

[4]. Tang RJ, Li FS, Shen FL, et al. Fast Forecasting of Water-Filled Bodies Position Using Transient Electromagnetic Method Based on Deep Learning. IEEE Transactions on Geoscience and Remote Sensing 2024; 62: 4502013. https://doi.org/10.1109/TGRS.2024.3355543

[5] Chen J, Zhang Y, and Lin TT. High-Resolution Quasi-Three-Dimensional Transient Electromagnetic Imaging Method for Urban Underground Space Detection. IEEE Transactions on Industrial Informatics 2023; 19(3): 3039-3046. https://doi.org/10.1109/TII.2022.3176890

[6] Witherly K, Irvine R, and Godbout M. Reid Mahaffy test site, Ontario Canada: An example of benchmarking in air-borne geophysics. In: Proc. 74th Annu. Int. Meeting, Soc. Explor. Geophysicists, Denver, CO, USA, Oct 2004, pp. 1202–1204. https://doi.org/10.1190/1.1843294

[7] Zhu X, Su X, Tai HM, et al. Bipolar steep pulse current source for highly inductive load. IEEE Trans. Power Electron 2016; 31(9): 6169–6175. https://doi.org/10.1109/TPEL.2015.2503383

[8] Wang Q, Wang H, Wu M, et al. Research on Noise Suppression Methods for Transient Electromagnetic Signal. In: IEEE Advanced Information Management, Communicates, Electronic and Automation Control Conference (IMCEC), 2018, pp. 394-397. https://doi.org/10.1109/IMCEC.2018.8469591

[9] Yu C, Fu Z, Wu G, et al. Configuration Detection of Substation Grounding Grid Using Transient Electromagnetic Method. IEEE Transactions on Industrial Electronics 2017, 64(8): 6475-6483. https://doi.org/10.1109/TIE.2017.2682033

[10] Qin SQ, Wang Y, Xu Z, et al. Fast Resistivity Imaging of Transient Electromagnetic Using ANN. IEEE Geoscience and Remote Sensing Letters 2019; 16(9): 1373-1377. https://doi.org/10.1109/LGRS.2019.2900992

[11] Gang Z, Rui X, Yu C, et al. Research on Double Coil Pulse Eddy Current Thickness Measurement. In: 2017 10th International Conference on Intelligent Computation Technology and Automation (ICICTA), 2017, pp. 406-409. https://doi.org/10.1109/ICICTA.2017.97

[12] Shi X and Tao F. Research on the detection of the high-resistivity body by transient electromagnetic method. In: Proceedings 2011 International Conference on Transportation, Mechanical, and Utilityal Engineering (TMEE), 2011, pp. 1103-1106. https://doi.org/10.1109/TMEE.2011.6199397

[13] Svatos J and Vedral J. The Usage of Frequency Swept Signals for Metal Detection. IEEE Transactions on Magnetics 2012,48(4): 1501-1504. https://doi.org/10.1109/TMAG.2011.2173174

[14] Tie CJ, Weng CC, Aydiner AA., et al. Detection of buried targets using a new enhanced very early time electromagnetic (VETEM) prototype system. IEEE Transactions on Geoscience and Remote Sensing 2001; 39(12): 2702-2712. https://doi.org/10.1109/36.975004

[15] Chang JH, Su BY, Malekian R, et al. Detection of Water-Filled Mining Goaf Using

Mining Transient Electromagnetic Method. IEEE Transactions on Industrial Informatics 2019; 16(5): 2977-2984.
https://doi.org/10.1109/TII.2019.2901856

[16] Qi ZP, Li X, Li H, et al. First Results from Drone-Based Transient Electromagnetic Survey to Map and Detect Unexploded Ordnance. IEEE Geoscience and Remote Sensing Letters 2020; 17(12): 2055-2059.
https://doi.org/10.1109/LGRS.2019.2962754

[17] Dentith, M., & Mudge, S. T. (2015). Geophysics for the mineral exploration geoscientist. Cambridge: Cambridge University Press.